Dielectric Constant Tunability at Microwave Frequencies and Pyroelectric Behavior of Lead-Free Submicron-Structured $(Bi_{0.5}Na_{0.5})_{1-x}Ba_xTiO_3$ Ferroelectric Ceramics

F. L. Martínez, J. Hinojosa, G. Doménech, F. J. Fernández-Luque, J. Zapata, R. Ruiz, and L. Pardo[1]

***Abstract*—In this article we show that the dielectric constant of lead-free ferroelectric ceramics based on the solid solution $(1-x)(Bi_{0.5}Na_{0.5})TiO_3$-$xBaTiO_3$, with compositions at or near the morphotropic phase boundary (MPB), can be tuned by a local applied electric field. Two compositions have been studied, one at the MPB, with x=0.06 (BNBT6), and another one towards the BNT side of the phase diagram, with x=0.04 (BNBT4). The tunability of the dielectric constant is measured at microwave frequencies between 100 MHz and 3 GHz by a non-resonant method and simultaneously applying a DC electric field. As expected, the tunability is higher for the composition at the MPB (BNBT6), reaching a maximum value of 60 % for an electric field of 900 V/cm, compared with the composition below this boundary (BNBT4), which saturates at 40 % for an electric field of 640 V/cm. The high tunability in both cases is attributed to the fine grain and high density of the samples, which have a submicron homogeneous grain structure with grain size of the order of a few hundred nanometers. Such properties make these ceramics attractive for microwave tunable devices. Finally, we have tested**

[1] This work was supported by Ministerio de Ciencia e Innovación of Spain (TIN2009-14372-C03-02), Fundación Séneca (15303/PI/10), and CSIC (PIE 201060E069).

F. L. Martínez, J. Hinojosa, G. Domenech, F. J. Fernández-Luque, J. Zapata and R. Ruiz are at the Departamento de Electrónica y Tecnología de Computadoras, Universidad Politécnica de Cartagena, E-30202 Cartagena, Spain.

L. Pardo is at the Instituto de Ciencias de Materiales de Madrid, Consejo Superior de Investigaciones Científicas, E-28049 Madrid, Spain.

these ceramics for their application as infrared pyroelectric detectors and we have found that the pyroelectric figure of merit is comparable to traditional lead containing pyroelectrics.

Keywords: ferroelectric ceramics; dielectric permittivity; microwave tunable devices; pyroelectric infrared sensors.

I. INTRODUCTION

Since the discovery of ferroelectric ceramics by the middle of the 20th century, $Pb(Zr,Ti)O_3$ (PZT) perovskite has been the most used ferro-piezoelectric material [1]. The reason for the success of PZT is intimately related to the morphotropic phase boundary (MPB) between the tetragonal and rhombohedral phases [2], which increases the number of equivalent directions of the spontaneous polarization of the crystal, P_s, and consequently increases also the remanent polarization P_r. However, an increased concern about the risks of the use of lead has promoted an intense effort to develop lead-free piezoelectric ceramics with properties that could match those of PZT. Since the coexistence of the two phases is considered to be at the origin of the high piezoelectric coefficients of PZT with compositions near the MPB, an alternative material has been sought that would present a similar behavior. Sodium bismuth titanate $(Na_{0.5}Bi_{0.5})TiO_3$ (BNT) has emerged as a good alternative to PZT because it has a strong ferroelectricity at room temperature and a high Curie temperature (T_c= 320 ºC) [3, 4, 5, 6]. It also forms solid solutions with the tetragonal perovskite $BaTiO_3$ (BT), which results in a morphotropic phase boundary between the BT phase and the rhombohedral BNT phase. Hence, the material system $(1-x)Bi_{0.5}Na_{0.5}TiO_3$-$xBaTiO_3$ (that we call BNT_{1-x}-BT_x, or simply BNBT100x), has some very attractive properties, especially for compositions at or near the MPB, for which a significant enhancement of the dielectric response occurs [2]. The transition between the rhombohedral (BNT-rich) and tetragonal (BT-rich) phases occurs for x between 5 % and 7 %, depending on the sources [2, 4, 5, 6], so most studies take BNBT6 as the reference composition to study the behavior at the MPB.

However, the phase diagram of BNBT is very complex, showing many peculiarities that are not yet well understood and that include ferroelectric, relaxor and non-polar phases [2]. These peculiarities result in important differences between BNBT and PZT, which may be the possible reason why the piezoelectric properties of lead-free BNBT are inferior to those of PZT. The contribution of domain wall motion to the electromechanical properties of PZT can also be important, but unfortunately there are not yet reports of domain wall contributions in PZT and lead-free materials made under comparable conditions [2]. The studies published so far seems to indicate that contributions to the permittivity from the domain wall motion in BNT-BT are quantitatively similar to those of PZT, although the mechanism responsible for it is completely different.

Recently, fine grain submicron-structured ceramics of BNT-BT have been synthesized with compositions at the MPB (BNBT6) and shifted to the BNT side of the solid solution (BNBT4) [5, 6]. Processing of ceramics from nanopowders allows obtaining fine grain compounds that are of interest both for the basic studies of size effects in ferroelectrics and for their use as high-frequency ultrasonic transducers. The piezoelectric properties of these submicron structured materials have already been studied [5, 6], and the purpose of this article will be to contribute to the knowledge of these ceramics by two new complementary characterizations: their pyroelectric behavior and the tunability of their dielectric constant at microwave frequencies (100 MHz-3GHz). Both characterizations are useful for applications to devices in which we are interested: the pyroelectric response is used for infrared detectors, while the dielectric constant tunability can be applied to microwave tunable devices. The results will be compared to those of traditional lead-containing PZT, so that consequences about the applicability of BNT-BT to practical commercial devices will be obtained.

Very few studies exist so far about the pyroelectric behavior of BNBT and its possible application to pyroelectric infrared sensors [7, 8]. Usually the pyroelectric coefficient *p*' is determined from measurements of depolarization current, and then a characteristic pyroelectric relation is calculated from the equation:

$$F_c = \frac{p'}{\sqrt{\varepsilon_r}} \tag{1}$$

However, for the application of this material as an infrared sensor it is more realistic to measure directly the pyroelectric voltage or pyroelectric current when the sample is irradiated by a modulated infrared beam emitted by a calibrated blackbody source. In this case the modulated infrared illumination simulates the movement of an infrared source, such as a person passing by, which has to be detected by the sensor. Our purpose is to use these sensors as part of a wireless network that detects anomalous situations in the life of elderly people who are alone at home and may need assistance at some moments or situations of risk [9, 10, 11]. The main components of this system are movement detectors placed in every room of the house and sensitive to the electromagnetic radiation emitted by the human beings in the long-wavelength infrared range (8-14 μm). Pyroelectricity provides the most efficient way to detect infrared radiation for this application because pyroelectric detectors do not require power supply and therefore they do not increase the power consumption of the wireless motes. Additionally, and contrary to the generally more sensitive IR photonic detectors (photodiodes or photoconductive devices), they do not require cooling, which notably simplifies the installation and operation of the motes [9, 10, 11].

For these reasons an experimental setup has been built to test the pyroelectricity of the BNBT samples in conditions similar to the real application. As a source of IR radiation we have chosen a calibrated blackbody emitter. Previously, measurements of the power radiated by the blackbody were done with a thermopile for different distances and as a function of the blackbody temperature, in order to compare them with the power emitted by a person at the same distances, and find the conditions that more accurately simulate the intended application. Since pyroelectric detectors are sensitive only to variations of the incoming IR power, the movement of the object was simulated by an optical chopper modulated at low frequencies between 1 Hz and 100 Hz. The BNBT samples were metalized with electrically conductive silver and placed on a probe station where we could make contact to these electrodes. Then they were illuminated by the modulated black-body

radiation and the current produced by the change in spontaneous polarization was amplified by a low-noise current preamplifier and a lock-in amplifier. The response of the material was studied as a function of modulation frequency, and the results are compared with other traditional lead-containing dielectrics.

The second practical application of BNBT that has not yet been explored with enough detail is that of microwave tunable devices, including tunable oscillators, phase shifters, long-range phase-array radar, and pulse compression waveguides in directed energy systems [12]. In this field, the properties of fine grained submicron or nanostructured ceramics such as those considered in this study are particularly interesting. The dielectric constant of BNBT at microwave frequencies has only been studied in one publication until now, which used non-poled samples for their study [2, 13]. In that publication, an impedance analyzer was used to measure the permittivity until 1 GHz, and the dielectric resonator technique [14] was used to determine the complex dielectric constant at some discrete frequencies above 3 GHz. In our case we will use a broad-band electromagnetic characterization technique of materials at microwave frequencies, involving *S*-parameter measurements, a specific measuring cell and an extraction method of the permittivity and permeability. A vector network analyzer is used to measure the *S*-parameters from the measuring cell. Among the different broad-band measuring cells available in the literature, the open-ended coaxial probe adjusts well to the characterization of disk-shaped samples [15, 16]. Other techniques such as measurements in free space require large dimensions of the samples at low microwave frequencies [17], while measurements with box-shaped cells need manufacturing processes for inserting the samples within the cell [18, 19, 20] and measurements with coplanar or microstrip cells involve technological processes for depositing metal on the samples [21, 22, 23]. In comparison, the open-ended coaxial probe allows nondestructive characterizations of different size materials from S_{11}^{*} reflection coefficient measurements.

In the following we present the experimental details and results from tests performed for both types of applications (pyroelectric and microwave), as applied to fine grain submicron-structured BNBT4 and BNBT6 samples described previously in the literature [5, 6].

II. EXPERIMENTAL SETUPS

A. Pyroelectric characterization.

We have tested BNBT as a pyroelectric sensor in realistic conditions similar to those that are used to test commercial pyroelectric detectors (PIRs). For this purpose we have built the experimental setup shown in Figure 1.

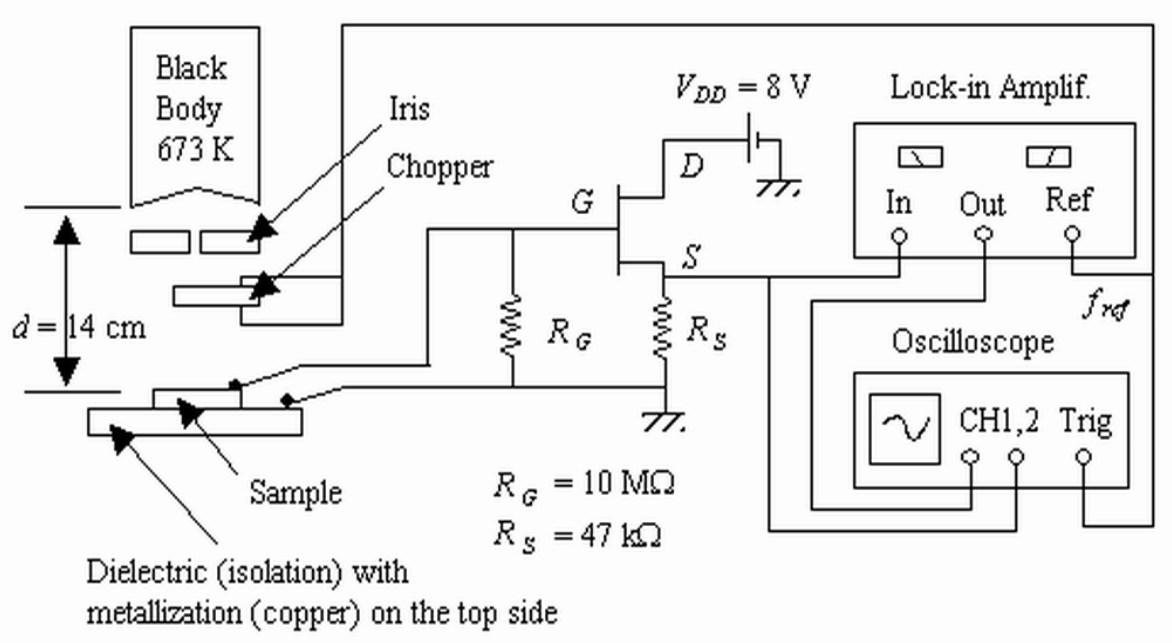

Fig. 1. Experimental setup for the measurement of the pyroelectric characteristics.

A calibrated blackbody radiation source is used as the infrared emitter. This allows us to have a constant and reproducible source of infrared radiation. The emission of the blackbody is passed through an iris that allows adjusting the level of infrared power incident on the sample. A chopper modulates this beam at a frequency that can be controlled between 2 Hz and 400 Hz. The sample is placed on a copper plate to allow a good electrical contact to the back electrode. Contact is made with needle probes on a Cascade Summit 9000 probe station. The pyroelectric voltage is measured using a lock-in amplifier which is frequency locked to the signal, hence eliminating most sources of noise. In the experiments presented here a JFET

source follower is placed between the sample and the amplifier in order to approach the conditions existing in a passive infrared sensor, where this transistor provides the necessary impedance matching to the detection circuit.

The emission of the infrared blackbody source has been first compared to that of a human being in order to select the cavity temperature that more accurately approaches the infrared emissions of a person. For this purpose we have used a Moll thermopile to measure the radiating power of the blackbody source at different distances, and we have compared it with the measurements of the radiating power of a person and of a movable self-made broad-area radiating oven at the same distances. The reason for the movable oven is to have at our disposition an infrared source that could be moved freely around a living lab, simulating the movements of an ill or elderly person being monitored by non-intrusive infrared detectors which should detect situations of risk [9, 10, 11]. The blackbody source turned out to be not appropriate for this purpose because it is a directional energy emitter, while a person emits infrared radiation in all directions. Our home-made oven is made of a cylindrical homogeneously heated black surface, which radiates uniformly in all directions. After calibration of the temperature of this oven, so that it will approach as much as possible the emitting power of a person, and doing a similar calibration of the blackbody cavity temperature, we obtained the results shown in Figure 2 for the detected power as a function of distance. The data follow an exponential decay law at distances larger than 1 m, indicating that the absorption of the infrared light in air prevails over the dependence of the expanding beam power density with the inverse square of the distance. However, at short distances below 1 m the tendency separates from the exponential decay law, indicating that in this short range the inverse quadratic law is predominant. The experiment also shows that the broad area uniform omni-directional oven simulates better the emission characteristics of a person at distances larger than 1.5 m, while at distances lower than 1 m the blackbody source provides a more realistic model. Hence the oven will be used in experiments related to signal analysis of PIRs networks aimed at extracting

information from different patterns of movements [9, 10, 11], while the blackbody source will be used in characterization of materials candidates for integrated lead-free pyroelectric sensors.

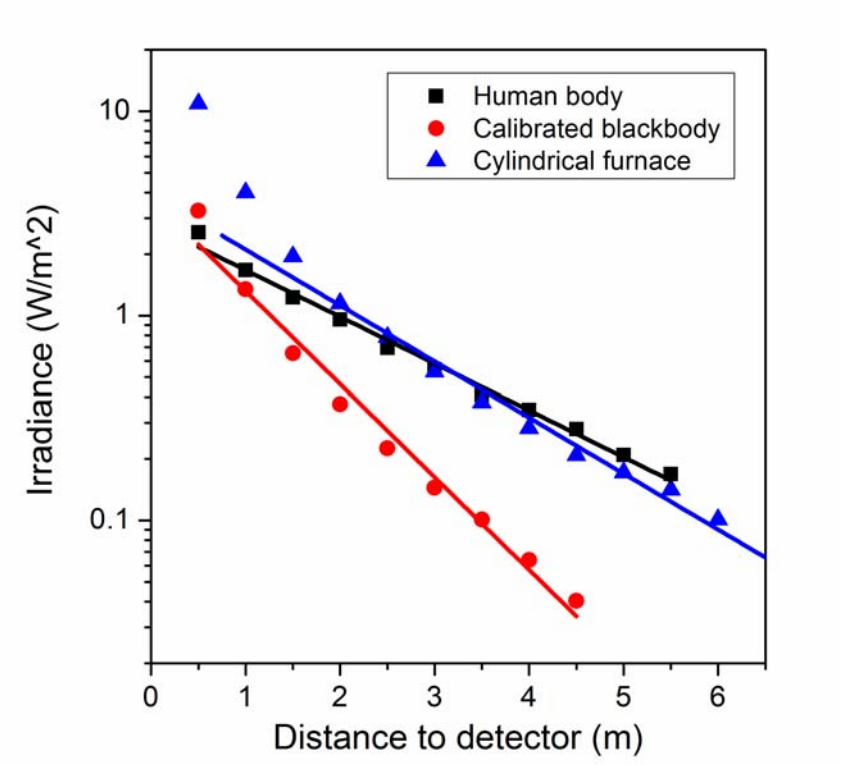

Media-Color Fig2

Fig. 2. Dependence of irradiated power with distance for a blackbody direccional source, an omni-directional cylindrical emitter and a person.

B. Microwave characterization

The dielectric constant at microwave frequencies of BNBT has only been measured in one published work until now [2]. As mentioned in the introduction, non-poled samples were used in that work and the measurements below 1 GHz were carried out with an impedance analyzer [13]. For frequencies between 3.3 and 7.8 GHz only some discrete frequencies were measured using the composite dielectric resonator technique [14]. For the application of BNBT to microwave tunable devices is necessary to test the response of the dielectric constant to an applied electric field at microwave frequencies. This section first describes

the measuring cell, the experimental setup and the extraction method of the complex permittivity that we have used to get the dielectric properties of ferroelectric BNBT4 and BNBT6 high density submicron structured ceramics [5, 6] at microwave frequencies, without and with applied DC bias electric fields. The parameters describing the tunability characteristic are also presented.

1) Measuring Cell and Experimental Setup

Two types of non-resonant methods can be used for the broad-band characterization of disk-shaped materials with coaxial lines: reflection/transmission method and reflection method. The reflection/transmission method involves inserting the material to be characterized within a portion of the coaxial transmission line. In addition to the manufacturing processes for adjusting the sample within the coaxial line, and thereby to minimize the air gaps, this technique is inaccurate if the electrical length of the sample cell is lower than several multiples of one-half of the guided wavelength [23]. Therefore, a very long coaxial transmission line is needed to cover the low microwave frequencies (< 3 GHz). On the other hand, the reflection method allows accurate broad-band measurements of materials in this microwave low frequencies range (< 3 GHz). Two types of reflection methods with different terminations can be used: open-reflection method and shorted-reflection method. The last one is used to measure magnetic permeability, while the first one is sensitive to the measurements of permittivity and, therefore, adequate for the ceramic samples that we want to characterize. This measuring cell is usually called coaxial dielectric probe. It allows nondestructive measurements of different size materials. The permittivity of the material under test is obtained from measurements of S_{11} reflection parameter with the coaxial dielectric probe.

The experimental setup is shown in Fig. 3. The measurements of the S_{11}^{*} reflection parameters are carried out by means of a vector network analyzer (VNA: Agilent Technologies E5070B) covering 300 kHz – 3 GHz. A radial DC electric field is applied to the sample under test by means of a DC source and a bias tee.

The reference plane P_1 is obtained from an initial calibration procedure (100 MHz – 3 GHz) using standard open and short terminations and a standard material with known dielectric permittivity [15, 16].

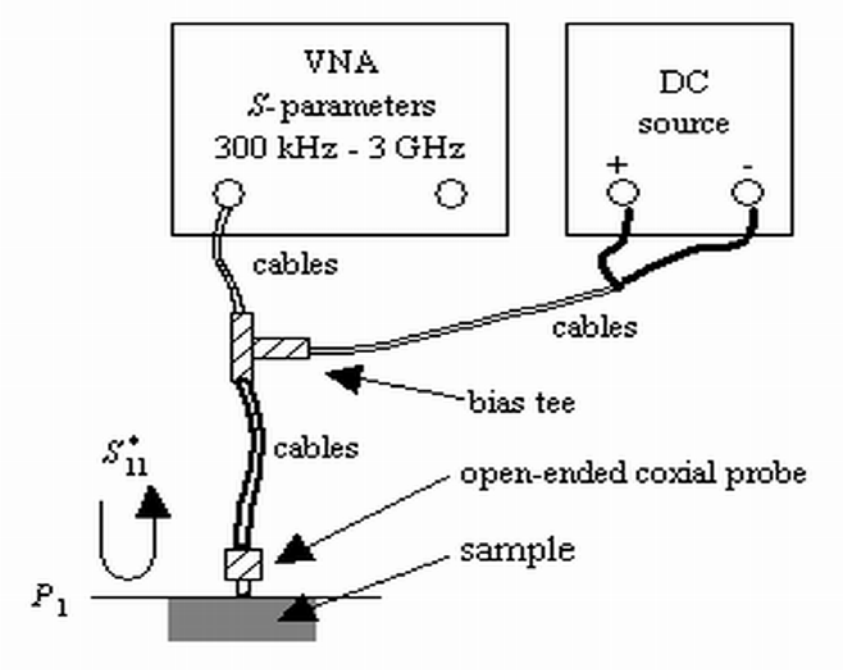

Fig. 3. Block diagram of the measurement setup.

2) Extraction Method of the Complex Permittivity

The complex permittivity is extracted from S_{11}^* parameter measurements performed at the interface P_1 between the coaxial probe and the sample under test, together with the analysis of the open-ended coaxial probe modeled by a simple equivalent circuit (Fig. 4) [15]. The reflection coefficient S_{11}^* is obtained at the reference plane P_1 by considering the complex admittance of the equivalent circuit:

$$S_{11}^* = \frac{1 - j\omega Z_0 (C(\varepsilon_r^*) + C_f)}{1 + j\omega Z_0 (C(\varepsilon_r^*) + C_f)} \tag{2}$$

where Z_0 is the characteristic impedance of the coaxial transmission line, ω is the angular frequency, C_f is a capacitance independent of the material under test and $C(\varepsilon_r^*) = \varepsilon_r^* C_0$ is the capacitance filled with the material under test (C_0 is the capacitance filled with air). C_f and C_0 are unknown and are determined by calibrating the coaxial open-ended probe with a standard material (*sm*) of known dielectric permittivity $\varepsilon_{r\,sm}^* = \varepsilon_{r\,sm}^{'} + j\varepsilon_{r\,sm}^{''}$:

$$C_0 = \frac{1 - \left|S_{11\,sm}^*\right|^2}{\omega Z_0 \left(1 + 2\left|S_{11\,sm}^*\right| \cos(\phi_{S_{11\,sm}}) + \left|S_{11\,sm}^*\right|^2\right) \varepsilon_{r\,sm}^{''}} \tag{3}$$

$$C_f = \frac{-2\left|S_{11\,sm}^*\right| \sin\left(\phi_{S_{11\,sm}}\right)}{\omega Z_0 \left(1 + 2\left|S_{11\,sm}^*\right| \cos(\phi_{S_{11\,sm}}) + \left|S_{11\,sm}^*\right|^2\right)} - \varepsilon_{r\,sm}^{'} C_0 \tag{4}$$

where $S_{11\,sm}^*$ is the complex reflection coefficient at the reference plane P_1, and $\phi_{S_{11\,sm}}$ is the phase of $S_{11\,sm}^*$. After calculating these capacitances, we can extract the complex dielectric permittivity of the sample under

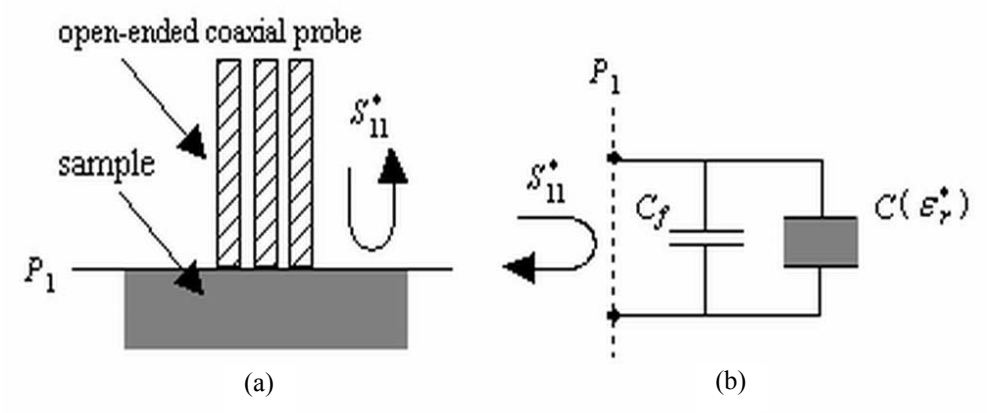

Fig. 4. Open-ended reflection method. (a) Open-ended coaxial probe loaded with a sample. (b) Capacitive equivalent circuit.

test from the values of S_{11}^* :

$$\varepsilon_r^* = \frac{1 - S_{11}^*}{j\omega Z_0 C_0 (1 + S_{11}^*)} - \frac{C_f}{C_0} \tag{5}$$

3) Tunability

The main feature of ferroelectric materials for microwave engineering applications is the dependence of their dielectric permittivity ε_r with an applied DC bias electric field *E*. This characteristic is commonly described by the tunability parameter *n* and by the relative tunability parameter n_r :

$$n = \frac{\varepsilon_r(0)}{\varepsilon_r(E)} \tag{6}$$

$$n_r = \frac{\varepsilon_r(0) - \varepsilon_r(E)}{\varepsilon_r(0)} = 1 - \frac{1}{n} \tag{7}$$

where $\varepsilon_r(0)$and $\varepsilon_r(E)$ correspond to the dielectric permittivity of the material at zero electric field and at some non-null electric field, respectively.

III. RESULTS AND DISCUSSION

A. *Pyroelectric results*

The pyroelectric voltage measured in the way described by the experiment of Figure 1 is presented in Figure 5 for the BNBT4 sample and compared with two other ferroelectric materials: lead titanate (PT) with 24 % substitution of Pb by Ca, and PT with 8 % substitution of Pb by Sm. It is known from previous work with pyroelectric detectors that the ratio of the pyroelectric coefficient to the square root of the permittivity is fairly constant for many pyroelectric materials [8, 24]. Hence, even though significant differences may

exist in the pyroelectric coefficient, the difference in the performance of pyroelectric detectors based on those materials is less significant. The relevant figure of merit (F_V) for comparing the pyroelectric voltage frequency response is the ratio of pyroelectric coefficient to permittivity and volume specific heat [25]. The theory that takes into account both the electrical and thermal impedances of the detector predicts a maximum of the responsivity (pyroelectric voltage divided by input power) at low frequencies, and an f^{-1} dependence proportional to the figure of merit at higher frequencies [25, 26]. The measurements shown in Fig. 3 match well this behavior for the three samples analyzed, as demonstrated by the good apparent linear fits of the pyroelectric voltage versus frequency on the logarithmic scales above the cutoff frequency determined by the electrical and thermal time constants [25].

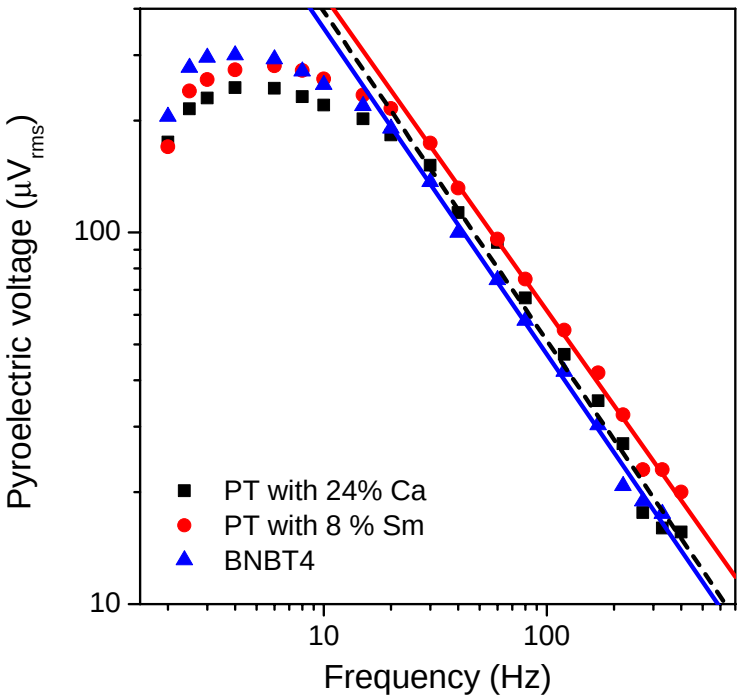

Media-Color Fig5

Fig. 5. Pyroelectric voltage as a function of frequency. Lines are apparent linear fits.

This is in agreement with previously published models of pyroelectric devices, which describe the frequency response in terms of two time constants: an electrical time constant (τ_E) related to the capacity of the pyroelectric element and a thermal time constant (τ_T) related to the thermal capacity (H) and thermal

conductance (G_T) to the surroundings. The value of the sensitivity of the sensor (R_v) is determined by the pyroelectric coefficient (p') and the values of these constants, which depend not only on the material used but also on its geometrical dimensions. Since all three tested samples received the same power of infrared illumination and produced similar values of pyroelectric voltage, it is concluded that the ratio $p'/(\tau_E+\tau_T)$ is comparable for the three pyroelectric elements that were characterized [25]. Since the geometrical dimensions were also similar for all of them (disks of 1.5 cm of diameter and thickness between 0.5 mm and 1.5 mm) it is concluded that the material parameters must be also similar, although the exact influence of each of them on the sensitivity requires further analysis and specialized measurements.

B. Microwave dielectric characterization results

The technique proposed in the experimental section has been used to measure the complex permittivity of BNBT4 and BNBT6 ceramics without and with applied DC bias electric fields in a range of frequencies covering 100 MHz – 3 GHz at room temperature (298 K). Figs. 6 and 7 show the measured $\varepsilon_r^{'}$ values as a function of frequency and the relative tunability (n_r) at 1 GHz for BNBT4 and BNBT6, respectively. The losses of this material are small and it has not been possible to measure their magnitude accurately by this technique.

As it can be seen in Fig. 6, BNBT4 presents significant dielectric constant variation with the applied DC bias electric field, while the $\varepsilon_r^{'}$ values decrease only slightly as a function of frequency. The higher values of the real part of the permittivity are obtained when no DC bias electric field is applied to the sample. At the frequency of 1 GHz, the BNBT4 ceramic material exhibits a $\varepsilon_r^{'}$ value equal to 26.3 for E = 0, which decreases down to a saturation value around $\varepsilon_r^{'}$=15 for an applied DC bias electric field higher than E = 600

V/cm. The change in permittivity as a function of applied DC bias electric field allows achieving a relative tunability of approximately 43 %.

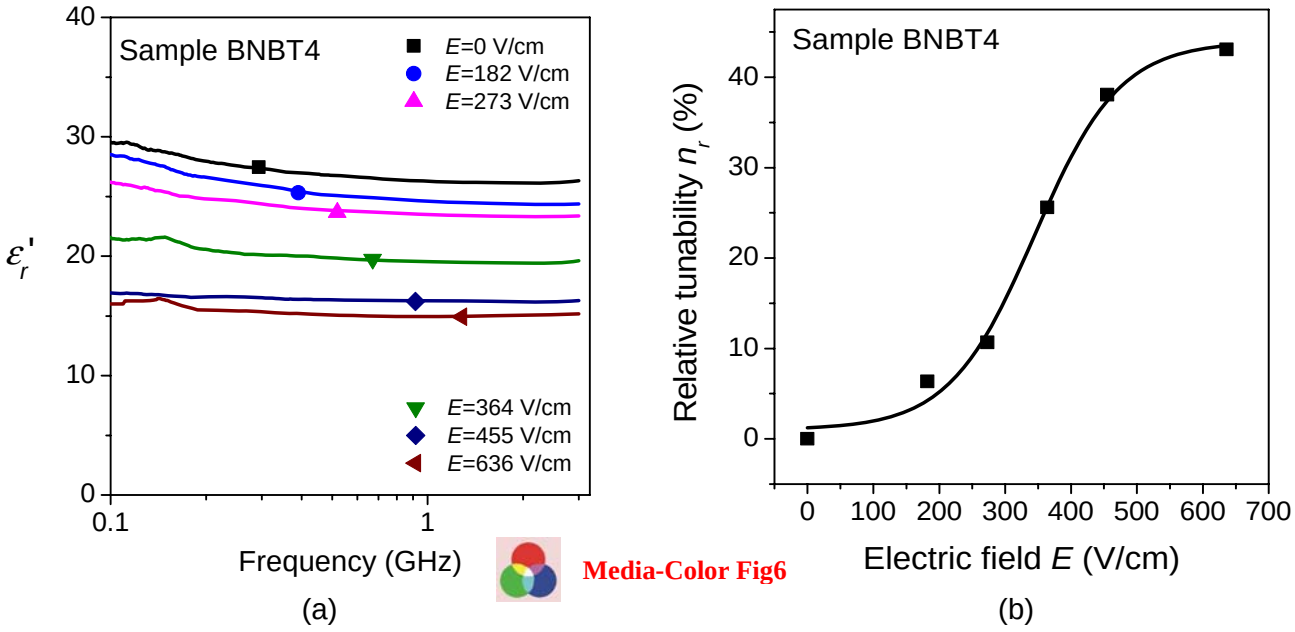

Fig. 6. Measured ε_r' data (a) and relative tunability (b) at *f*=1 GHz for the BNBT4 ceramic material.

If we compare the values of dielectric constant and relative tunability of the BNBT4 sample (Fig. 6) with those of BNBT6 (Fig. 7), we observe that at the morphotropic phase boundary composition (100*x*=6) the dielectric constant is significantly higher: $\varepsilon_r' = 35.8$ for *E*=0 (compared to 26.3 for the composition 100*x*=4, below the MPB). The relative tunability is also larger for the BNBT6 sample, because it reaches a value of 60 % for electric fields around 730 V/cm. For larger electric fields the tunability saturates in that value, corresponding to a dielectric constant of $\varepsilon_r' = 14$ at the frequency of 1 GHz. This means that the saturation value of the dielectric constant is approximately the same for the two compositions.

The higher values of tunability at the morphotropic phase boundary are consistent with the enhanced dielectric properties at that composition. A high density submicron structure is generally associated with higher tunability values [27, 28], which may explain the results obtained for these ceramics. Previously

published results of microwave tunability refer mostly to single phase systems [28], specially (Ba,Sr)TiO_3 single crystals and ceramics [27], so that direct comparison with a two-phase system at the MFB is not straight-forward. The high dielectric constants and the large range of tuning for the BNBT ceramics can be of interest for the development and design of novel compact tunable microwave devices

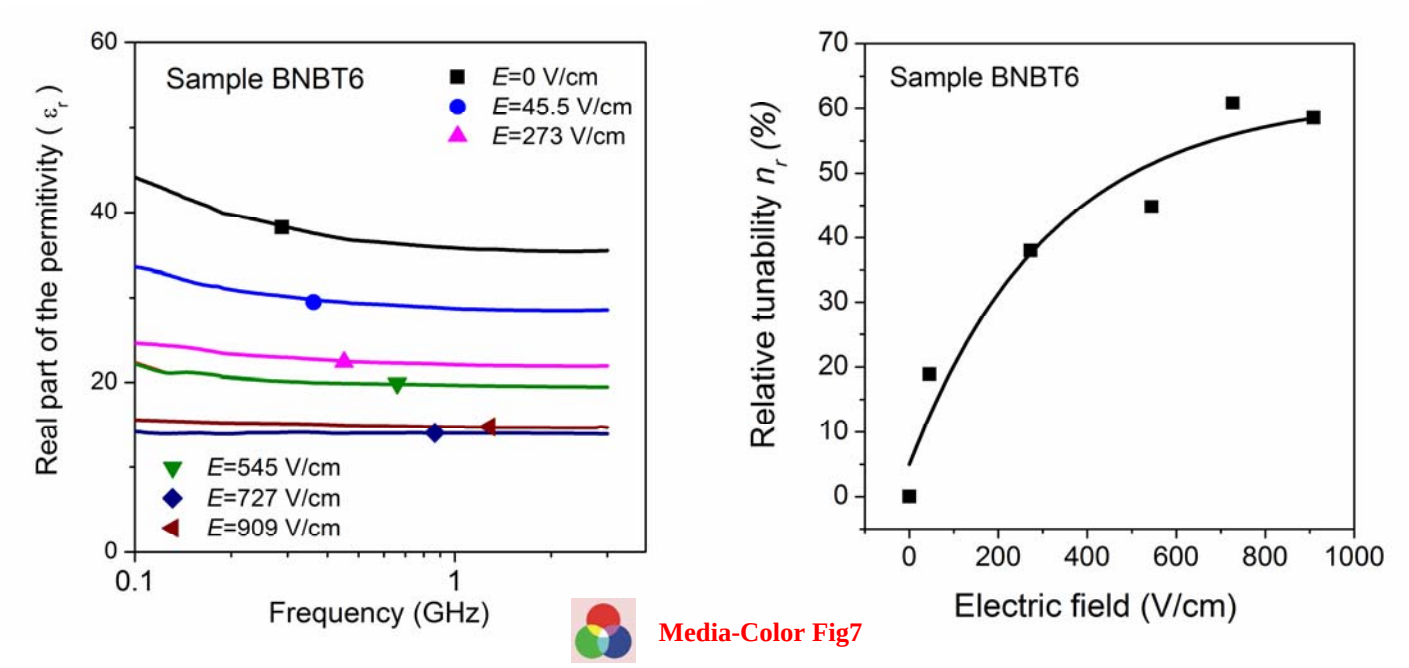

(a) (b)

Fig. 7. Measured ε_r' data (a) and relative tunability (b) at *f*=1 GHz for the BNBT6 ceramic material

IV. CONCLUSION

The application of lead-free submicron structured BNBT ceramics to two types of devices (pyroelectric detectors and microwave tunable devices) has been studied. In the first case, a pyroelectric voltage has been measured with a test experiment designed to characterize passive infrared sensors in conditions that simulate real working conditions. The results have been comparable to traditional lead-containing dielectrics (PZT),

both in the magnitude of the detected pyroelectric voltage and in its dependence with the frequency of the modulated excitation source.

In the second study (application to microwave tunable devices), the modulation of the dielectric permittivity with a locally applied DC electric field seems to be promising, although here too further studies are necessary to bridge the gap between low frequency measurements (below 5 MHz) based on impedance analyzers or capacitance meters, and microwave measurements based on resonant [2, 13, 14] or non-resonant methods (such as the one presented here). Since the study of fine grain submicron-structured solid solutions of BNBT is still on an early stage, and many properties of this material are still not well understood, we hope that progress will continue and realization of devices based on this material will become possible.

REFERENCES

[1] G. H. Haertling, "Ferroelectric Ceramics: History and Technology", *J. Am. Ceram. Soc.*, vol. 82, no.4, pp.797-818, 1999.

[2] D. Damjanovic, N. Klein, J. Li, and V. Porokhonskyy, "What can be expected from lead-free piezoelectric materials?", *Functional Materials Letters*, vol. 3, no. 1, pp. 5-13, 2010.

[3] D. Alonso-Sanjosé, R. Jiménez, I. Bretos, and M. L. Calzada, "Lead-free ferroelectric $Na_{1/2}Bi_{1/2}TiO_3$-$BaTiO_3$ thin films in the morphotropic phase boundary composition: solution processing and properties", *J. Am. Ceram. Soc.*, vol. 92, no. 10, pp. 2218-2225, 2009.

[4] L. Pardo, A. García, K. Brebol, L. P. Curecheriu, L. Mitoseriu, E. Mercadelli, and C. Galassi, "Piezoelectric characterization of lead-free ferroelectric ceramics", *Processing and Application of Ceramics*, vol. 4, no. 3, pp. 199-207, 2010.

[5] L. Pardo, A. García, K. Brebol, E. Mercadelli, and C. Galassi, "Piezoelectric properties of lead-free sumicron-structured $(Bi_{0.5}Na_{0.5})_{0.94}Ba_{0.06}TiO_3$ ceramics from nanopowders", *Smart Mater. Struct.*, vol. 19, pp. 115007(1-10), 2010.

[6] L. Pardo, A. García, K. Brebol, E. Mercadelli, and C. Galassi, "Enhanced properties for ultrasonic transduction, phase transitions and thermal depoling in $0.96(Bi_{0.5}Na_{0.5})TiO_3$-$0.04BaTiO_3$ submicrometre-structured ceramics", *J. Phys. D: Appl. Phys.*, vol. 44, pp. 335404(1-9), 2011.

[7] Y. Guo and M. Gu, "Antiferroelectric phase and pyroelectric response in $(Na_yBi_z)Ti_{1-x}O_{3(1-x)}$-$x$$BaTiO_3$ ceramics", *J. Am. Ceram. Soc.*, vol. 94, no. 5, pp. 1350-1353, 2011.

[8] R. Rodríguez-Ruiz, R. González-Ballesteros, A. Flores-Cuautle, and E. Suaste-Gómez, "Determination of the pyroelectric coefficient for $(Bi_{0.5}Na_{0.5})_{0.935}Ba_{0.065}TiO_3$ piezoelectric ceramics", *Ferroelectrics*, vol. 368, pp. 216-223, 2008.

[9] R. Paoli, F. J. Fernández-Luque, G. Doménech, F. Martínez, J. Zapata, and R. Ruiz, "A system for ubiquitous fall monitoring at home via a wireless sensor network and a wearable mote", *Expert Systems with Applications*, vol. 39, pp. 5566-5575, 2012.

[10] F. J. Fernández-Luque, F. Martínez, G. Ginés Doménech, J. Zapata, and R. Ruiz, "EMFi-based low-power occupancy sensor", *Sensors and Actuators A: Physical*, vol. 191, pp. 78-88, 2013.

[11] F. J. Fernández-Luque, D. Pérez, F. Martínez, G. Doménech, I. Navarrete, J. Zapata, and R. Ruiz, "An energy efficient middleware for an ad-hoc AAL wireless sensor network", *Ad Hoc Networks*, http://dx.doi.org/10.1016/j.adhoc.2012.10.003.

[12] J. de los Santos, D. García, and J. A. Eiras, "Dielectric Characterization of Materials at Microwave Frequency Range", *Materials Research*, vol. 6, no. 1, pp. 97-101, 2002.

[13] N. Klein, PhD Thesis no. 4528, Swiss Federal Institute of Technology – EPFL (2009).

[14] Jerzy Krupka, T. Zychowicz, V. Bovtun, and S. Veljko, “Complex Permittivity Measurements of Ferroelectrics Employing Composite Dielectric Resonator Technique”, *IEEE Transactions on Ultrasonics, Ferroelectrics and Frequency Control*, vol. 53, no. 10, pp. 1883-1888, 2006.

[15] T. W. Athtey, M. A. Stuchly, and S. S. Stuchly, “Measurement of radio frequency permittivity of biological tissues with an open-ended coaxial line: Part I”, *IEEE Trans. Microwave Theory Tech.*, vol. 30, no. 1, pp. 82-86, Jan. 1982.

[16] M. A. Stuchly, T. W. Athtey, C. M. Samaras, and G. E. Taylo, “Measurement of radio frequency permittivity of biological tissues with an open-ended coaxial line: Part II”, *IEEE Trans. Microwave Theory Tech.*, vol. 30, no. 1, pp. 87-91, Jan. 1982.

[17] D. K. Ghodgaonkar, V. V. Varadan, and V. K. Varadan, “Free-space measurement of complex permittivity and complex permeability of magnetic materials at microwave frequencies”, *IEEE Trans. Instrum. Meas.*, vol. 39, no. 2, pp. 387-394, Apr. 1990.

[18] W. B. Weir, “Automatic measurement of complex dielectric constant and permeability at microwave frequencies”, *Proc. IEEE*, vol. 62, no. 1, Jan. 1974.

[19] N.-E. Belhadj-Tahar, A. Fourier-Lamer, and H. De Chanterac, “Broad-band simultaneous measurement of complex permittivity and permeability using a coaxial discontinuity”, *IEEE Trans. Microwave Theory Tech.*, vol. 38, no. 1, pp. 1-7, Jan. 1990.

[20] N. K. Das, S. M. Voda, and D. M. Pozar, “Two methods for the measurement of substrate dielectric constant”, *IEEE Trans. Microwave Theory Tech.*, vol. 35, no. 7, pp. 636-642, Jul. 1987.

[21] J. Hinojosa, “S-parameter broadband measurements on-coplanar and fast extraction of the substrate intrinsic properties”, *IEEE Microwave Wireless Compon. Lett.*, vol. 11, no. 2, pp. 80-82, Feb. 2001.

[22] J. Hinojosa, “S-parameter broadband measurements on-microstrip and fast extraction of the substrate intrinsic properties”, *IEEE Microwave Wireless Compon. Lett.*, vol. 11, no. 7, pp. 305-307, Jul. 2001.

[23] J. Hinojosa, “Permittivity characterization from open-end microstrip line measurements”, *Microwave Opt. Technol. Lett.*, vol. 30, no. 6, pp. 1371-1374, Jun. 2007.

[24] S. T. Liu, J.D. Zook, and D. Long, “Relationships between pyroelectric and ferroelectric parameters”, *Ferroelectrics*, vol. 9, no. 1, pp. 39-43, Jan. 1975.

[25] R. W. Whatmore, “Pyroelectric devices and materials”, *Rep. Prog. Phys.*, vol. 49, pp. 1335-1386, 1986

[26] E. H. Putley, “A method for evaluating the performance of pyroelectric detectors”, *Infrared Physics*, vol. 20, no. 3, pp. 139-147, May 1980.

[27] S. Kwon, W. Hackenberger, E. Alberta, E. Furman, and M. Lanagan, “Nonlinear dielectric ceramics and their applications to capacitors and tunable dielectrics”, *IEEE Electrical Insulation Magazine*, vol. 27, no. 2, pp. 43-55, 2011.

[28] A. K. Tagantsev, V. O. Sherman, K. F. Astafiev, J. Venkatesh, and N. Setter, “Ferroelectric materials for microwave tunable applications”, *Journal of Electroceramics*, vol. 11, pp. 5-66, 2003.